

AD/A-005 777

**RHEOLOGY OF CONCENTRATED SUSPENSIONS
OF FIBERS IN TUBE FLOW: III.
SUSPENSIONS WITH THE SAME FIBER
LENGTH DISTRIBUTION**

Richard O. Maschmeyer, et al

Monsanto Research Corporation

Prepared for:

**Office of Naval Research
Advanced Research Projects Agency**

December 1974

DISTRIBUTED BY:

NTIS

**National Technical Information Service
U. S. DEPARTMENT OF COMMERCE**

AD/A-005777

Security Classification		DOCUMENT CONTROL DATA - R & D	
(Security classification of title, body of abstract and indexing annotation must be entered when the overall report is classified)			
1. ORIGINATING ACTIVITY (Corporate author)		2a. REPORT SECURITY CLASSIFICATION	
Monsanto Research Corporation		Unclassified	
		2b. GROUP	
3. REPORT TITLE			
Rheology of Concentrated Suspensions of Fibers in Tube Flow: III. Suspensions with the Same Fiber Length Distribution			
4. DESCRIPTIVE NOTE 5 (Type of report and inclusive dates)			
6. AUTHOR(S) (First name, middle initial, last name)			
Richard O. Maschmeyer and Christopher T. Hill			
7. REPORT DATE		7a. TOTAL NO. OF PAGES	7b. NO. OF REFS
December, 1974		36	
8a. CONTRACT OR GRANT NO		9a. ORIGINATOR'S REPORT NUMBER(S)	
N00014-67-C-0218		HPC-74-170	
b. PROJECT NO			
c.		9b. OTHER REPORT NO(S) (Any other numbers that may be assigned this report)	
d.			
10. DISTRIBUTION STATEMENT			
Approved for public release; distribution unlimited.			
11. SUPPLEMENTARY NOTES		12. SPONSORING MILITARY ACTIVITY	
		Office of Naval Research Washington, D. C.	
13. ABSTRACT			
<p>Capillary viscometer measurements were made on a series of concentrated suspensions with the same fiber length distribution. Shear stress-shear rate data are reported for 0, 15, and 30 vol.% glass fiber suspensions in 100, 600, and 1000 P silicone oil. Yield stresses, wall effects, concentration defects, squeeze-through, and capillary entrance exclusion were not significant in the measurements.</p> <p>With other parameters held constant, the suspension viscosity increased with oil viscosity. The data were fit by a dimensionless plot of the form $F(fRe, De) = 0$ where f is the friction factor for tube flow and Re and De are the Reynolds and Deborah numbers of the system. The suspension viscosity increased with fiber concentration, but the magnitude of the increase was highly shear rate dependent. The data are compared with literature predictions for the dependence of suspension viscosity on fiber concentration and shear rate.</p>			

14

KEY WORDS

Rheology
 Suspensions
 Fibers
 Viscosity
 Non-Newtonian
 Capillary Rheometer
 Mixing
 Dimensional Analysis

LINK A

LINK B

LINK C

ROLE

WT

ROLE

WT

ROLE

WT

ia

RHEOLOGY OF CONCENTRATED SUSPENSIONS OF FIBERS IN TUBE FLOW:

III. SUSPENSIONS WITH THE SAME FIBER LENGTH DISTRIBUTION

by

Richard O. Maschmeyer and Christopher T. Hill
Materials Research Laboratory
Washington University
St. Louis, Missouri 63130

December 1974

Monsanto/Washington University Association
High Performance Composites Program
Sponsored by ONR and ARPA
Contract No. N00014-67-C-0218, ARPA Order 876

Approved for Public Release: Distribution Unlimited.

The views and conclusions contained in this document are those of the authors and should not be interpreted as necessarily representing the official policies either expressed or implied of the Advanced Research Projects Agency or the U.S. Government.

FOREWORD

The research reported herein was conducted by the staff of Monsanto/Washington University Association under the sponsorship of the Advanced Research Projects Agency, Department of Defense, through a contract with the Office of Naval Research, N00014-67-C-0218 (formerly N00014-66-C-0045), ARPA Order No. 876, ONR contract authority NR 356-484/4-13-66, entitled "Development of High Performance Composites".

The prime contractor is Monsanto Research Corporation. The Program Manager is Dr. Rolf Buchdahl (Phone 314-694-4721).

The contract is funded for \$7,000,000 and expires 30 June, 1974.

RHEOLOGY OF CONCENTRATED SUSPENSIONS OF FIBERS IN TUBE FLOW:

III. SUSPENSIONS WITH THE SAME FIBER LENGTH DISTRIBUTION

Richard O. Maschmeyer and Christopher T. Hill
Materials Research Laboratory
Washington University
St. Louis, Missouri 63130

ABSTRACT

Capillary viscometer measurements were made on a series of concentrated suspensions with the same fiber length distribution. Shear stress-shear rate data are reported for 0, 15, and 30 vol.% glass fiber suspensions in 100, 600, and 1000 P silicone oil. Yield stresses, wall effects, concentration defects, squeeze-through, and capillary entrance exclusion were not significant in the measurements.

With other parameters held constant, the suspension viscosity increased with oil viscosity. The data were fit by a dimensionless plot of the form

$$F(fRe, De) = 0$$

where f is the friction factor for tube flow and Re and De are the Reynolds and Deborah numbers of the system. The suspension viscosity increased with fiber concentration, but the magnitude of the increase was highly shear rate dependent. The data are compared with literature predictions for the dependence of suspension viscosity on fiber concentration and shear rate.

RHEOLOGY OF CONCENTRATED SUSPENSIONS OF FIBERS IN TUBE FLOW:

III. SUSPENSIONS WITH THE SAME FIBER LENGTH DISTRIBUTION

I. INTRODUCTION

Part I (1) of this series reviewed the sparse experimental literature on the rheological properties of concentrated fiber suspensions in tube flow. Little agreement about the rheological properties was found among various researchers. Part II (2) reported the results of an exploratory study of concentrated fiber suspensions in which a strong dependence of rheology on fiber length distribution was observed. The separate effects of fiber concentration, oil viscosity, and fiber length distribution on suspension viscosity were difficult to measure because these variables are compounded during mixing. This paper describes the results of viscosity measurements on a series of suspensions, all of which had the same fiber length distribution.

II. VISCOSITY THEORIES

In order to make comparisons with our data, we review briefly the theoretical studies which provide explicit expressions for viscosity applicably to concentrated fiber suspensions in tube flow. Brodnyan (3) predicted:

$$\eta_r = \exp \left\{ \frac{2.5\phi + 0.399 (r_p - 1)^{1.48} \phi}{1 - k\phi} \right\} \quad (1)$$

In this equation η_r is the reduced viscosity, ϕ is the volume fraction, r_p is the length-to-diameter ratio of the fibers, and k is a crowding factor. The numbers 0.399 and 1.48 are constants which were evaluated empirically. Even for the data Brodnyan used to evaluate the numerical constants, the equation will fit the data only up to 0.5 vol.%.

More recently, Ziegel (4) derived:

$$\eta_r = \left(\frac{3\mu Z\beta}{\dot{\gamma}} + 1 - Z \right) \frac{r_p^{5/3} \phi}{9.668} + 1 \quad (2)$$

where μ is an interaction or closeness-of-approach parameter, β is a rate constant for the equilibrium between free particles and agglomerates, and Z is the degree of agglomeration. Only the shear rate dependence of the equation was tested in Ziegel's paper and the test was only over a shear rate range of one and a half orders of magnitude.

Hashin (5) used the flow-elasticity analogy to predict:

$$\eta_r = 1 + \frac{2\phi}{1-\phi} \quad (3)$$

This equation is expected to be valid only for parallel, randomly placed, infinitely long fibers. Nielsen (6) used the same analogy, with the Halpin-Tsai equation, to predict:

$$\eta_r = \frac{1 + (k-1)B\phi}{1 - \psi\phi} \quad (4)$$

where

$$\psi = 1 + \left(\frac{1-\phi_m}{\phi_m^2} \right) \phi$$

$$B = \frac{\eta_{\text{part}}/\eta_o - 1}{\eta_{\text{part}}/\eta_o^{-k+1}}$$

$$K = \lim_{\phi \rightarrow 0} \eta_r - 1$$

where ϕ_m is the maximum possible volume fraction. The quantity B is very nearly unity for rigid particles in a viscous medium. To the authors' knowledge, the equation has never been tested for concentrated fiber suspensions.

III. EXPERIMENTAL TECHNIQUES

The extruder mixing technique and the capillary viscometer used for viscosity measurements in this study were described in detail elsewhere (2). The same fiber length distribution was produced in all suspensions by utilizing the fact that, with additional mixing, the suspensions approached an "ultimate state of mixedness" beyond which continued mixing at the same conditions did not change the suspensions' properties. The suspensions used in this study were mixed as follows. The viscosities of all silicone oils were nearly equalized by changing the temperature of the extruder. This step ensured that all suspensions with the same fiber concentration would have the same fiber length distribution after mixing. The suspensions of highest concentration were then mixed to their "ultimate state of mixedness" (six passes through the extruder were required). Suspensions of lower concentration were made without changing the fiber length distribution by blending the high concentration suspensions with additional oil and extruder mixing.

The mixing procedure afforded little independent control over the fiber length distribution produced; but, as the log-normal distribution statistics in Table I show, the distribution was nearly the same in all suspensions. Figure 1 shows a typical fiber histogram; the mean fiber length is 0.005" and the median length is 0.01".

IV. SUSPENSION PARAMETER

We believe Table 2 lists all the suspension parameters (as opposed to flow parameters) which determine the viscosity of a concentrated suspension of fibers. The values of fiber diameter, modulus, and Poisson ratio listed in Table 2 are manufacturers' specifications. Since these values are common to all our suspensions, their independent determination was felt to be unnecessary.

The values of the remaining parameters were measured as follows. The suspensions were mixed by weight, so the fiber concentration was determined at the time of mixing. The actual concentration achieved was verified for selected suspensions by Soxhlet extraction of the oil. Compressibility measurements indicated the amount of residual trapped air (the third phase of major concern) was less than 0.12 vol.-%--a negligible amount. In numerous microscopic examinations, the silicone oil was observed always to wet the glass fibers and the fibers were observed always to be separated from their original bundled configuration. These observations indicate negligible surface effects and random dispersion of fibers. The fiber orientation is believed to be random as a result of the high shear in the extruder.

The oil viscosities as functions of shear rate are shown in Figures 5-7. The oils show non-Newtonian behavior at high shear rates. Possible changes in the oil viscosity during mixing, due either to degradation or to evaporation of the low molecular weight fraction, were monitored by centrifuging the oils from the suspensions and measuring their viscosities. Although the viscosities did appear to change a few percent, experimental difficulties in removing all the glass particles made the results ambiguous (7). The suspected changes were small and no correction was made for them in our data.

V. EXPERIMENTAL RESULTS

As shown in Table 3, no differences in suspension viscosity or entrance pressure losses were observed when the entrance angle of the viscometer was changed from 180° to 90° . This result has been observed before (8-10) and is presumably due to the formation of a stagnant region in the 180° entrance such that the effective angle is closer to 90° . All other measurements reported in this paper were made with the 90° entrance angle.

Shear stress-apparent shear rate data for the suspensions are plotted in Figures 2-4. The symbols in these figures represent $\pm 6\%$ error flags, which constitute one standard deviation in our measurements. None of the suspensions exhibited a yield stress in the shear rate range measured as indicated by the absence of a horizontal asymptote at low shear rates. As may be seen in Figures 2-4, no differences between the flow curves measured in the $1/4''$ and $1/8''$ diameter capillaries were observed. This observation precludes the possibility of measurable wall effects, such as slip-at-the-wall, mechanical exclusion, or hydrodynamic interaction; probably due to the small fiber lengths relative to the tube diameters. The observation makes apparent viscosity a useful parameter for characterizing the flow of suspensions in tubes with diameters greater than $1/8''$. Apparent viscosity-apparent shear rate data are plotted in Figures 5-7.

Capillary entrance exclusion and squeeze-through were not observed to occur with any of the suspensions. The possible existence of a concentration defect was checked by comparing the capillary and exit concentrations of a suspension in the flow condition most likely to reveal a defect:

highest flow rate and longest capillary. No concentration defect was observed. These results are not surprising in view of the absence of measurable wall effects.

VI. DIMENSIONAL ANALYSIS

In order to discuss the effect of oil viscosity and fiber concentration on suspension viscosity, it is useful to apply dimensional analysis to our system. Dimensional analysis is possible with the aid of one assumption whose plausibility we shall now motivate. We restrict our analysis to suspensions with the same fiber length distribution and fiber concentration and to measurements made with the same viscometer. We treat the suspension as a continuous, two phase system of rigid fibers in a generalized Newtonian fluid and assume that only hydrodynamic forces operate. The system we wish to non-dimensionalize includes all of the suspension in the viscometer from the time the piston starts to move.

The major difficulty in dealing with this system is our lack of knowledge about the initial positions of the fibers where the boundary conditions for the problem are given. We have observed, however, that if different batches of the same suspension are run through the viscometer, the same force is always required to extrude at a given piston speed. (2) Since exact duplication of the initial fiber positions from batch to batch is highly improbable, we conclude that there must be many different initial distributions which are statistically equivalent as far as the average, macroscopic properties measured are concerned. This conclusion seems intuitively reasonable, for the initial fiber positions are presumed

random, and there are many possible random distributions. Furthermore, the distributions which are possible do not depend on the oil viscosity, so it seems reasonable that the distributions which are actually produced during mixing also may not depend on the oil viscosity (over a reasonable range of viscosities). We therefore assume that two well mixed suspensions with the same fiber length distributions and fiber concentrations but different oil viscosities have equivalent initial fiber position distributions. Equivalent in this sense means that the measured viscosities of the two suspensions would be experimentally indistinguishable if the suspending fluids were the same.

With the above assumption, all of the suspensions under consideration are geometrically similar. Dimensional analysis is possible since the dimensionless groups which characterize all the systems are the same. To determine the relevant dimensionless groups, we explicitly non-dimensionalize the equations of motion which describe our suspensions. Although any three-constant generalized Newtonian fluid model would be acceptable for the analysis, we choose for concreteness the Carreau model (11):

$$\eta(\dot{\gamma}; \eta_o, \dot{\gamma}_o, n) = \frac{\eta_o}{\left\{1 + (\dot{\gamma}/\dot{\gamma}_o)^2\right\}^{\frac{n-1}{2}}} \quad (5)$$

The Carreau model constants for the silicone oils used in this study are listed in Table 4. We assume that the constitutive equation which represents the fluid in viscometric flow will also serve to represent it in whatever flow occurs in the suspensions. Elastic effects in the silicone oils are negligibly small.

To non-dimensionalize the equations of motion, we introduce the following dimensionless variables:

$$\underline{v}^* = \underline{v}/V \quad P^* = \frac{P}{P_L - P_0} \quad t^* = \frac{tV}{D} \quad \underline{x}^* = x/D \quad (6)$$

where D is the capillary diameter, $P_L - P_0$ is the average pressure drop across the capillary, and V is the average flow rate through the capillary. The constitutive equation may be written:

$$\underline{\underline{\sigma}} = \frac{\eta_0 V}{D} h\left(\frac{V}{D\dot{\gamma}_0}, n, \dot{\gamma}^*\right) \underline{\underline{\dot{\gamma}}}^* \quad (7)$$

where h is a dimensionless function specified by the Carreau model. Neglecting both gravity and inertia, the equation of motion becomes:

$$0 = -EuRe \nabla^* P^* + \nabla^* \cdot h(De, n, \dot{\gamma}^*) \underline{\underline{\dot{\gamma}}}^* \quad (8)$$

The dimensionless groups $Eu = \frac{P_L - P_0}{\rho V^2}$, $Re = \frac{\rho DV}{\eta_0}$ and $De = \frac{V}{D\dot{\gamma}_0}$ are the Euler, Reynolds, and Deborah numbers, respectively, with their attendant physical meaning.

As shown in Table 4 the power law index, " n ", is nearly constant for the silicone oils, so we ignore explicit dependence on " n ". Dimensionless groups representing fiber concentration, diameter, and length distribution are not explicitly required because of the assumption that these quantities are constant for the suspensions considered. One additional dimensionless group, L/D , the ratio of length to diameter of the capillary, is necessary to meet the boundary conditions. The suspensions

are thus characterized by the three dimensionless groups $EuRe$, De , and L/D . Since the dimensionless groups form an Abelian group, we may choose a new basis for the group from among products of the old. Specifically,

$$\frac{1}{2} EuRe \left(\frac{L}{D}\right)^{-1} = fRe \quad (9)$$

where $f = \frac{1}{2} \left(\frac{D}{L}\right) \frac{P_L - P_0}{\rho v^2}$ is the friction factor commonly used in capillary flow. It is important to note that the group, fRe , arises only when inertia is negligible. Langlois (12) describes an alternative definition of P^* , appropriate when inertia is negligible, which leads directly to the group we call fRe . Finally, the end correction procedure allows us to treat fully developed flow only, so we may neglect L/D . The suspension flow at fixed fiber concentration is thus described by a relationship of the form:

$$F(fRe, De) = 0 \quad (10)$$

or

$$fRe = fRe(De) \quad (11)$$

VII. EFFECT OF OIL VISCOSITY ON SUSPENSION VISCOSITY

Figure 8 shows that unique curves of fRe versus De are indeed obtained, one curve for each of the three fiber concentrations. The symbols in Figure 8 represent $\pm 6\%$ error flags (one standard deviation). We believe the increased scatter in the 30 vol.% data is due to the small change in the viscosity of the oil which occurred during mixing--the 0 vol.% suspensions were not mixed and the 15 vol.% suspensions were diluted with pure, undegraded oil, so the change in viscosity shows up mostly in the 30 vol.% data.

We note that

$$fRe = \frac{2\sigma_w D}{\eta_o V} = \frac{16\sigma_w}{\eta_o \dot{\gamma}_a} = 16 \frac{\eta_a}{\eta_o} \quad (12)$$

and

$$De = \frac{V}{D \dot{\gamma}_o} = \frac{1}{8} \frac{\dot{\gamma}_a}{\dot{\gamma}_o} \quad (13)$$

so that Figure 8 may be interpreted as a plot of reduced apparent viscosity versus reduced apparent shear rate. The curves have the general form normally assumed by such plots for polymeric materials.

The only theory in the literature which predicts quantitatively the shear rate dependence of the viscosity of concentrated fiber suspensions is that of Ziegel (4). His theory does not fit our data.

VIII. EFFECT OF FIBER CONCENTRATION ON SUSPENSION VISCOSITY

The concentration dependence of suspension viscosity is normally presented by plotting reduced viscosity against concentration. As shown above, reduced apparent viscosity is an appropriate variable for describing our suspensions but it must be expected to depend on Deborah number. The reduced apparent viscosity-versus-concentration data for our suspensions are plotted in Figure 9 for various Deborah numbers. The reduced apparent viscosity is less than one at high De because it is referred to the zero-shear-rate viscosity of the oil. The curves resemble those reported by Newman and Tremontozzi (13) for different fiber suspensions.

As can be seen in Figure 9, the dependence of suspension viscosity on concentration is highly shear rate dependent. A qualitative understanding of the strong shear rate dependence may be gained from the dimensional

analysis discussed earlier. It is obvious from Figure 8 that the dimensionless group fRe depends on De . In other words, the silicone oil is not behaving as a Newtonian fluid despite that fact that the pure oil is Newtonian over most of the flow rate range considered. This result suggests that the apparent shear rate at the wall is a poor (low) measure of the actual shear rates occurring in the suspension, because the increased viscosity of a suspension over that of the pure fluid is associated with the disturbed velocity profile and higher shear rates in the fluid caused by the presence of the particle. Presumably these higher shear rates lower the non-Newtonian viscosity of the fluid around the particle. Hence, the resulting suspension viscosity is lower than would be expected if the fluid were Newtonian. This effect should be, and is, more pronounced at higher fiber concentrations and higher flow rates.

It appears in principle that the phenomenon could be strong enough that the apparent viscosity of a suspension might lie below the apparent viscosity of the pure oil at the same flow rate. Figure 8 suggests this might occur in our suspensions at shear rates slightly above the highest we were able to measure. The phenomenon could help explain the data of Thomas and Hagen (14), who observed suspension viscosities which were lower than that of pure resin and who explained the results as due to resin degradation. In a recent paper Charrier and Rieger (15) found very weak dependence of viscosity on fiber concentration in commercial glass-filled polypropylene, and they have invoked a similar mechanism to explain their observations.

The suspension theories of Brodnyan (3), Ziegel (4), Hashin (5) and Nielsen (6) provide equations which predict the dependence of reduced suspension viscosity on fiber concentration. Ziegel's theory predicts linear dependence of η_r on ϕ , which, as Figure 8 shows, is not exhibited by our suspensions. Comparison of the remaining equations with our data is difficult because these equations assume mono-disperse fibers and Newtonian oil behavior. We chose the median aspect ratio of 20:1 to represent the length of the fibers. The maximum allowed volume fraction for these fibers, as determined from centrifuging experiments, was 38 vol.%. The suspensions appear to exhibit a generalized Einstein coefficient, k , of 11.5. The equations using these values are plotted in Figure 10 and are compared with the data taken at the lowest shear rate, because the silicone oil is behaving most like a Newtonian fluid at low shear rates. Brodnyan's prediction at 30 vol.% is ten orders of magnitude too high and clearly does not fit the data. A similar conclusion was reached by Newman and Trenenozzi (13). Hashin's prediction is too low, but the use of his equation with our data is questionable because our suspensions do not meet his assumptions of parallel, infinitely long fibers. Nielsen's equation fits the data within experimental uncertainty.

IX. DISCUSSION OF THE DIMENSIONAL ANALYSIS

The dimensional analysis presented in this paper is not rigorous. The fact that it makes some interesting predictions about suspension flow which fit our data suggests that a more rigorous dimensional analysis might be worthwhile.

The very general analysis may be applied to viscometers of any geometry and to particles of any shape in suspensions of any concentration. However, the group $fRe \propto \eta_a/\eta_o$ arises only when inertia is negligible, which suggests that the reduced viscosity is an appropriate parameter for characterizing suspensions only in this case. The analysis also predicts that the shear rate dependence of η_a/η_o arises from De ; that is, from the non-Newtonian behavior of the suspending oil and not from changes in particle orientation as is commonly asserted.

However, two problems exist with the analysis as developed. First, the analysis is based on an assumption about the initial condition of the suspension in the barrel but the results of the analysis are applied to fully developed flow. This slight of hand only presents significant problems when we wish to neglect inertia. A good argument can be made for neglecting inertia in fully developed flow; what is needed is a clear statement of what is meant by neglecting inertia during start-up in the entry region of the viscometer.

A more rigorous statement of the basic assumption of statistically equivalent distributions of initial fiber positions is also needed. Some insight into the problem may be gained by considering the ensemble of all possible distributions as represented in Figure 11 for two suspensions, A and B, which differ only in oil viscosity. Both ensembles are identical because the initial fiber positions which are possible do not depend on the oil viscosity. Our data tells us that each ensemble contains a large subset comprising the initial distributions, the members of which are experimentally indistinguishable. These initial distributions are

contained in the curves of Figure 11. Typical extrusion force measurements on suspensions A and B will be made on some distributions which are members of the subset--call them A_1 and B_1 . The existence of these subsets are fundamental to reproducible viscosity measurements on suspensions without explicit control over particle orientation. The exact nature of the subsets presumably depends on the accuracy of the experiments. We assume that the two subsets have at least one common member--distribution 0 in Figure 11. This assumption is reasonable in view of the large number of distributions in each subset. The results of measurements on A_1 and B_1 are experimentally indistinguishable from A_0 and B_0 , and the latter may be rigorously compared by dimensional analysis. Thus we have some confidence that we can treat members such as A_1 and B_1 by the same analysis.

A. CONCLUSIONS

This paper described an experimental technique by which several suspensions with the same fiber length distribution but different oil viscosities and fiber concentration were mixed. The following conclusions apply to those suspensions in the range in which the measurements were made.

1. Wall effects and other special suspension effects were not detected.
2. Suspension viscosity was not dependent on capillary entrance angle or capillary diameter.

3. Suspension viscosity increased with oil viscosity and generally decreased with flow rate. The data fit a dimensionless plot of the form

$$F(fRe, De) = 0$$

which is essentially a plot of reduced apparent viscosity versus reduced apparent shear rate.

4. Suspension viscosity increased with fiber concentration, and the magnitude of the increase was highly shear rate dependent. One explanation of the shear rate dependence is the non-Newtonian behavior of the silicone oil.

ACKNOWLEDGMENT

This work was supported in part by ARPA Contract N00014-67-C-0218, formerly N00014-66-C-0045, and by NSF Grant No. GH 34594. We wish to acknowledge numerous useful discussions with Drs. L. E. Nielsen and B. A. Whipple.

REFERENCES

1. R. O. Maschmeyer and C. T. Hill, Advances in Chemistry, 134, 95-105 (1974).
2. R. O. Maschmeyer and C. T. Hill, Trans. Soc. Rheol., 00, 000-000 (1975).
3. J. Brodnyan, Trans. Soc. Rheol., 3, 61 (1959).
4. K. Ziegel, J. Coll. Int. Sci., 34, 185 (1970).
5. Z. Hashin, Contributions to Mechanics, (D. Abir, ed.) Pergamon Press, Oxford (1969).
6. L. Nielsen, J. Appl. Phys., 41, 4626 (1970).

7. R. Maschmeyer, D.Sc. Dissertation, Washington Univ., St. Louis, Missouri, 1974.
8. M. Takano, Report Number HPC 73-165, Monsanto/Washington University Association (1973).
9. J. Bell, J. Comp. Matl., 3, 244 (1969).
10. G. Stankoi, E. Trostyanskaya, Yu Kazanaki, V. Okorokov, and O. Mikhasenok, Soviet Plastics, 47 (September 1968).
11. P. Carreau, Ph.D. Dissertation, Univ. of Wisconsin, Madison (1968).
12. W. Langlois, Slow Viscous Flow, McMillan, New York (1964) 63-66.
13. S. Newman and Q. Tremontozzi, J. Appl. Poly. Sci., 9, 3071 (1965).
14. D. Thomas and R. Hagan, SPI, Reinforced Plast. Div., Annual Meeting (1966).
15. J.-M. Charrier and J.-M Rieger, Fibre Sci. Tech., 7, 161-172 (1974).

Table 1
Fiber Length Distributions of the Suspensions
(Uncertainties are two standard deviations)

Oil Viscosity (P)	Concentration (vol.%)	Mean Fiber Length (log _e inch)	Standard Deviation (log _e inch)
100	15	-5.38 ± 0.08	0.71 ± 0.07
100	30	-5.49 ± 0.08	0.71 ± 0.07
600	15	-5.30 ± 0.08	0.67 ± 0.07
600	30	-5.26 ± 0.08	0.66 ± 0.07
1000	15	-5.24 ± 0.08	0.68 ± 0.07
1000	30	-5.27 ± 0.08	0.66 ± 0.07

Table 2

Suspension Parameters which Determine Suspension Viscosity

Material Properties:

Oil Rheology:

Viscosity - 100, 600, 1000 P

Time dependent and elastic effects - negligible

Fiber Properties:

Length - same distribution in all suspensions

Diameter - 0.0005"

Youngs modulus - 10^7 psi

Poisson ratio - 0.2

Suspension Properties:

Concentration - 0, 15, 30 vol.%

Dispersion and Orientation - random

Third phases - none

Surface effects - negligible

Table 3
Effect of Viscometer Entrance Angle
(Uncertainties are One Standard Deviation)

Entrance Angle (°)	Shear Rate (sec ⁻¹)	Entrance Pressure Losses (dynes/cm ²)	Viscosity (P)
180	527	$6.3 \pm 1.3 \times 10^6$	960 ± 36
90	527	$7.3 \pm 0.6 \times 10^6$	940 ± 20

Table 4
Carreau Model Constants for the Silicone Oils

Nominal Viscosity (P)	η_0 (P)	$\dot{\gamma}_0$ (sec ⁻¹)	n
100	100	2300	0.70
600	600	400	0.67
1000	1000	240	0.67

CAPTIONS FOR FIGURES

1. Histogram of the fiber lengths in a typical suspension.
2. Shear stress-shear rate behavior of three suspensions of fibers in 100 P oil. The symbols (\bigcirc -1/4" cap.; \triangle -1/8" cap.) represent $\pm 6\%$ error flags.
3. Shear stress-shear rate behavior of three suspensions of fibers in 600 P oil. The symbols (\bigcirc -1/4" cap.; \triangle -1/8" cap.) represent $\pm 6\%$ error flags.
4. Shear stress-shear rate behavior of three suspensions of fibers in 1000 P oil. The symbols (\bigcirc -1/4" cap.; \triangle -1/8" cap.) represent $\pm 6\%$ error flags.
5. Viscosity-shear rate behavior of three suspensions of fibers in 100 P oil. The symbols (\bigcirc -1/4" cap.; \triangle -1/8" cap.) represent $\pm 6\%$ error flags.
6. Viscosity-shear rate behavior of three suspensions of fibers in 600 P oil. The symbols (\bigcirc -1/4" cap.; \triangle -1/8" cap.) represent $\pm 6\%$ error flags.
7. Viscosity-shear rate behavior of three suspensions of fibers in 1000 P oil. The symbols (\bigcirc -1/4" cap.; \triangle -1/8" cap.) represent $\pm 6\%$ error flags.
8. Dimensionless plot of fRe versus De at constant n . The symbol size represents $\pm 6\%$ error flags.
9. Reduced viscosity-concentration dependence of all suspensions at several Deborah numbers. The symbols have no significance as error flags.
10. Comparison of viscosity-concentration dependence at lowest Deborah number with literature predictions.
11. Representations of the ensembles of all possible initial fiber position distributions for two suspensions with different oil viscosities. Each small square represents a particular distribution. The distributions inside the closed curve are experimentally indistinguishable.

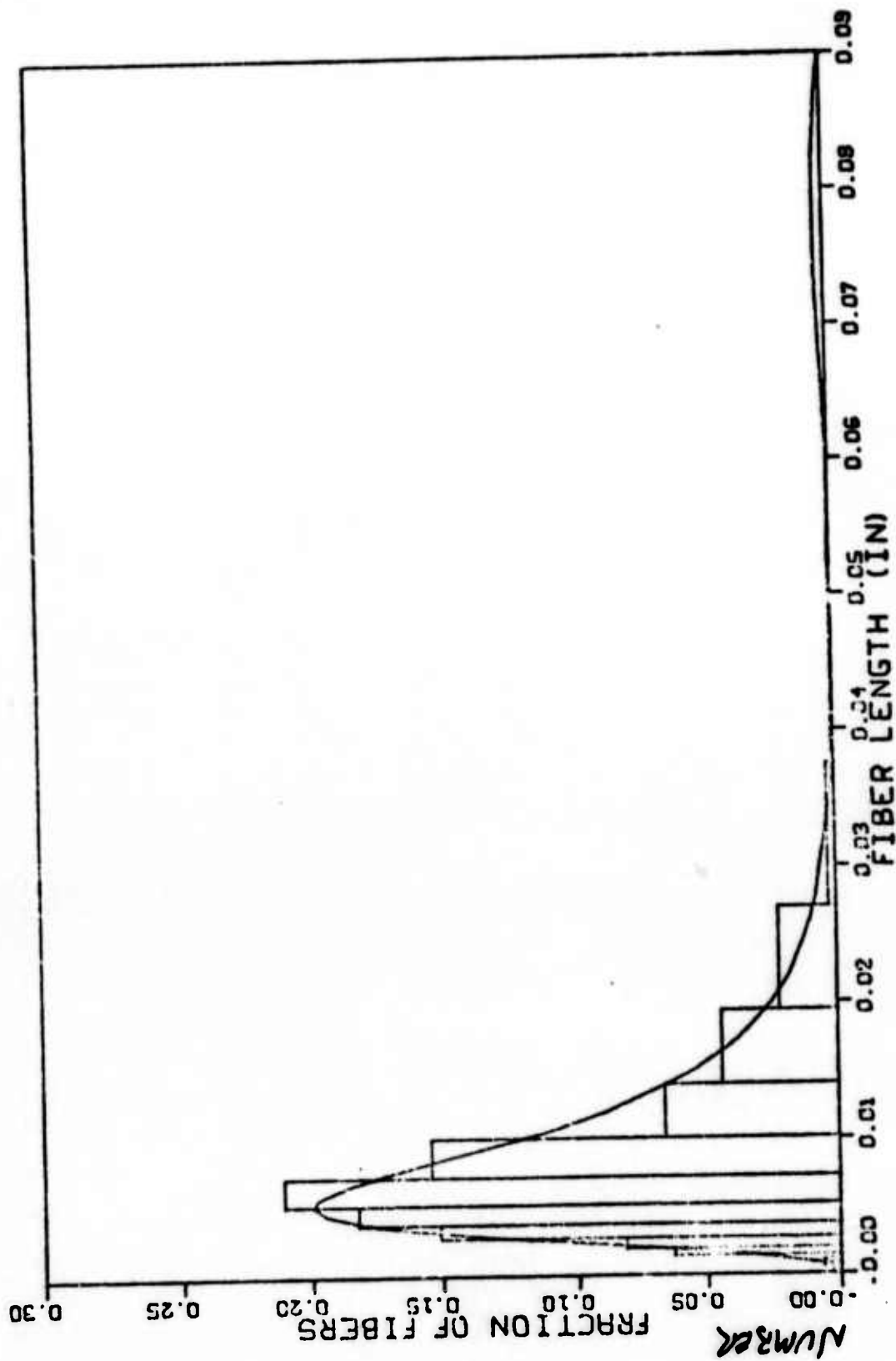


Figure 1 Histogram of suspension 30 vol.% 600 P - 63.

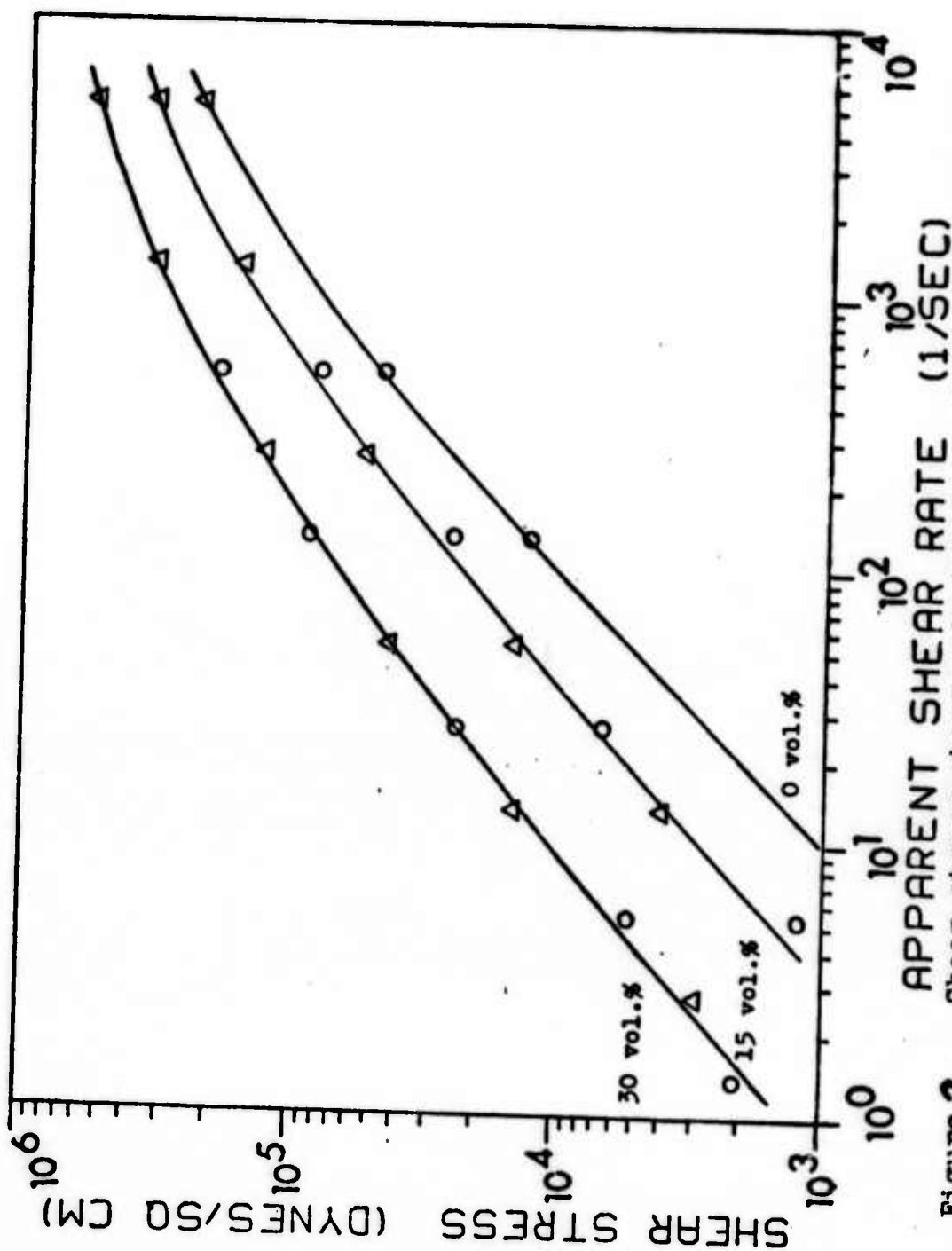


Figure 2 . Shear stress-shear rate behavior of three suspensions of fibers in 100 P oil. The symbols (\circ -1/4" cap.; Δ -1/8" cap.) represent $\pm 6\%$ error flags.

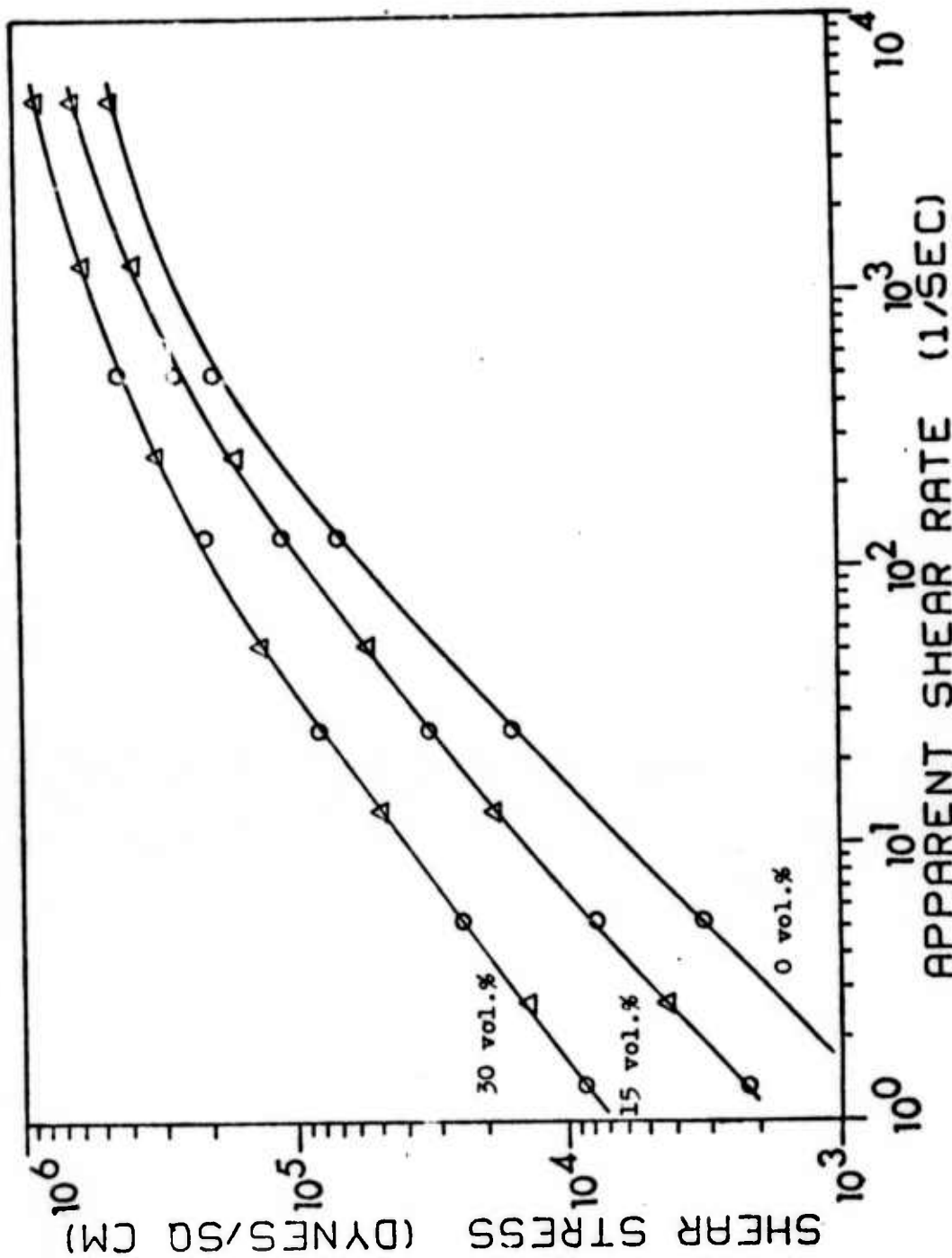


Figure 3 . Shear stress-shear rate behavior of three suspensions of fibers in 600 P oil. The symbols (\circ -1/4" cap.; Δ -1/8" cap.) represent $\pm 6\%$ error flags.

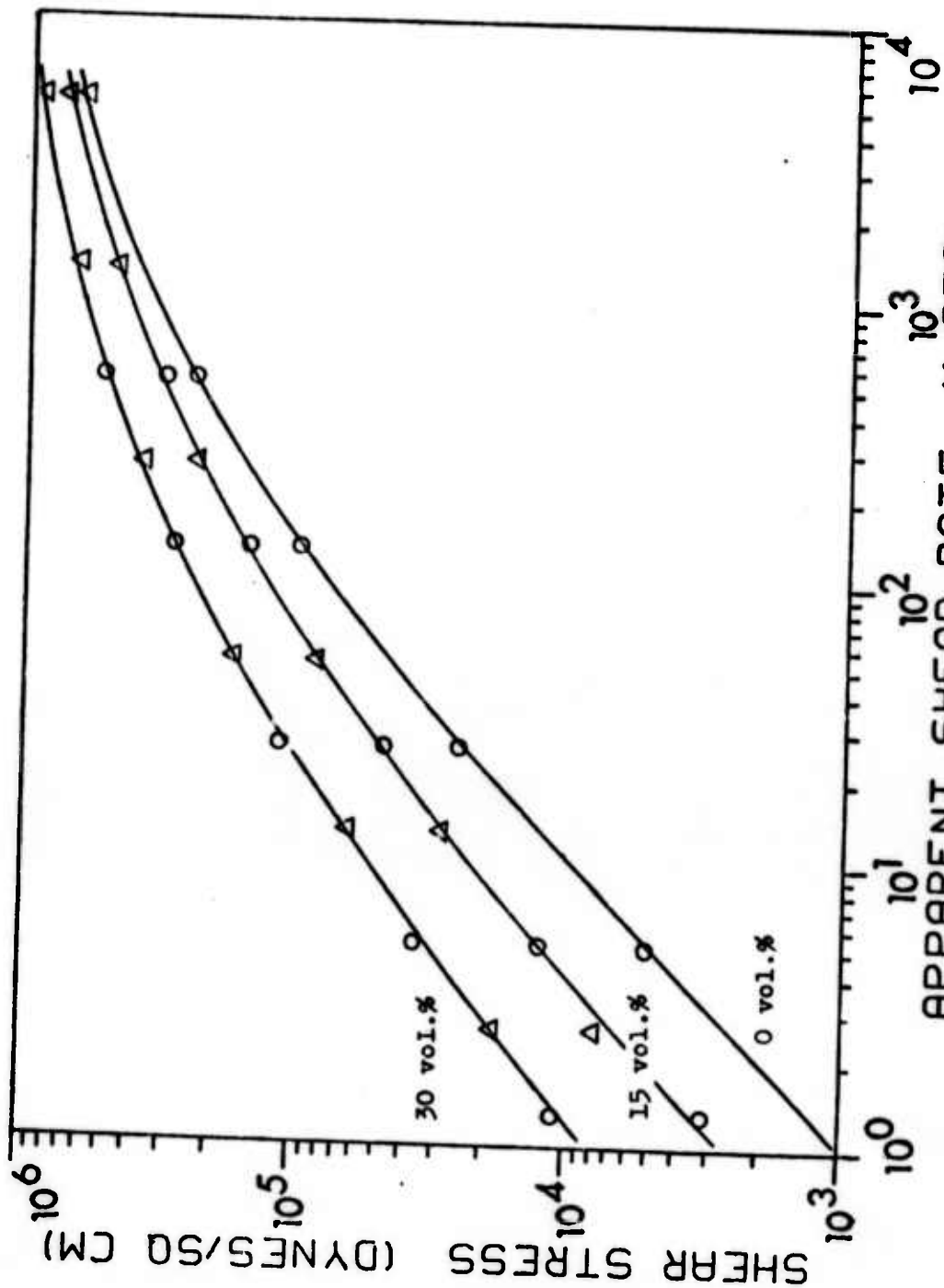


Figure 4 Shear stress-shear rate behavior of three suspensions of fibers in 1000 P oil. The symbols (O -1/4" cap.; Δ -1/8" cap.) represent $\pm 6\%$ error flags.

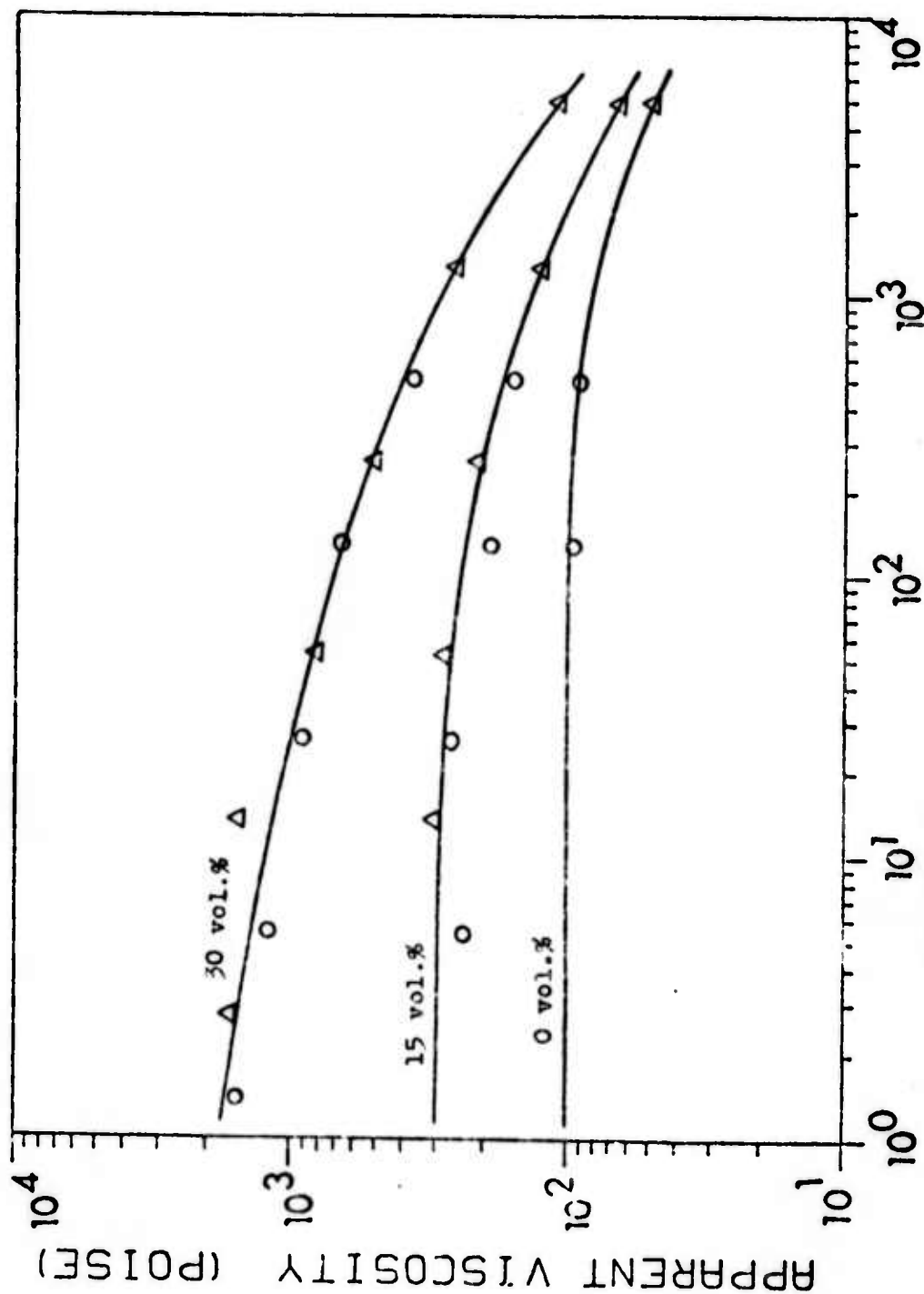


Figure 5 Viscosity-shear rate behavior of three suspensions of fibers in 100 P oil. The symbols (\circ , \triangle) represent $\pm 5\%$ error flags.

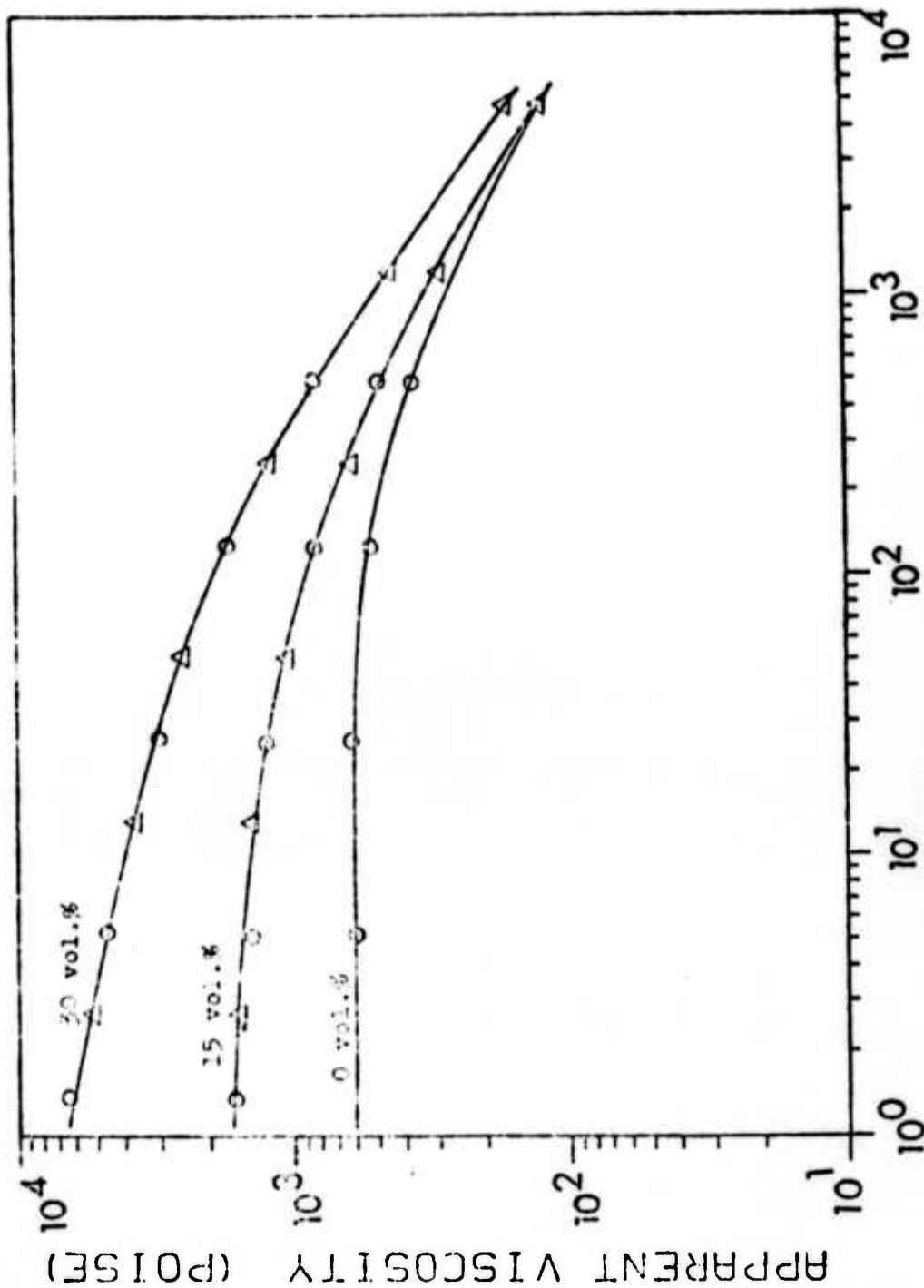


Figure 6 Viscosity-shear rate behavior of three suspensions of fibers in 600 P oil. The symbols ($-1/4$ " cap.; $-1/8$ " cap.) represent $\pm 6\%$ error flags.

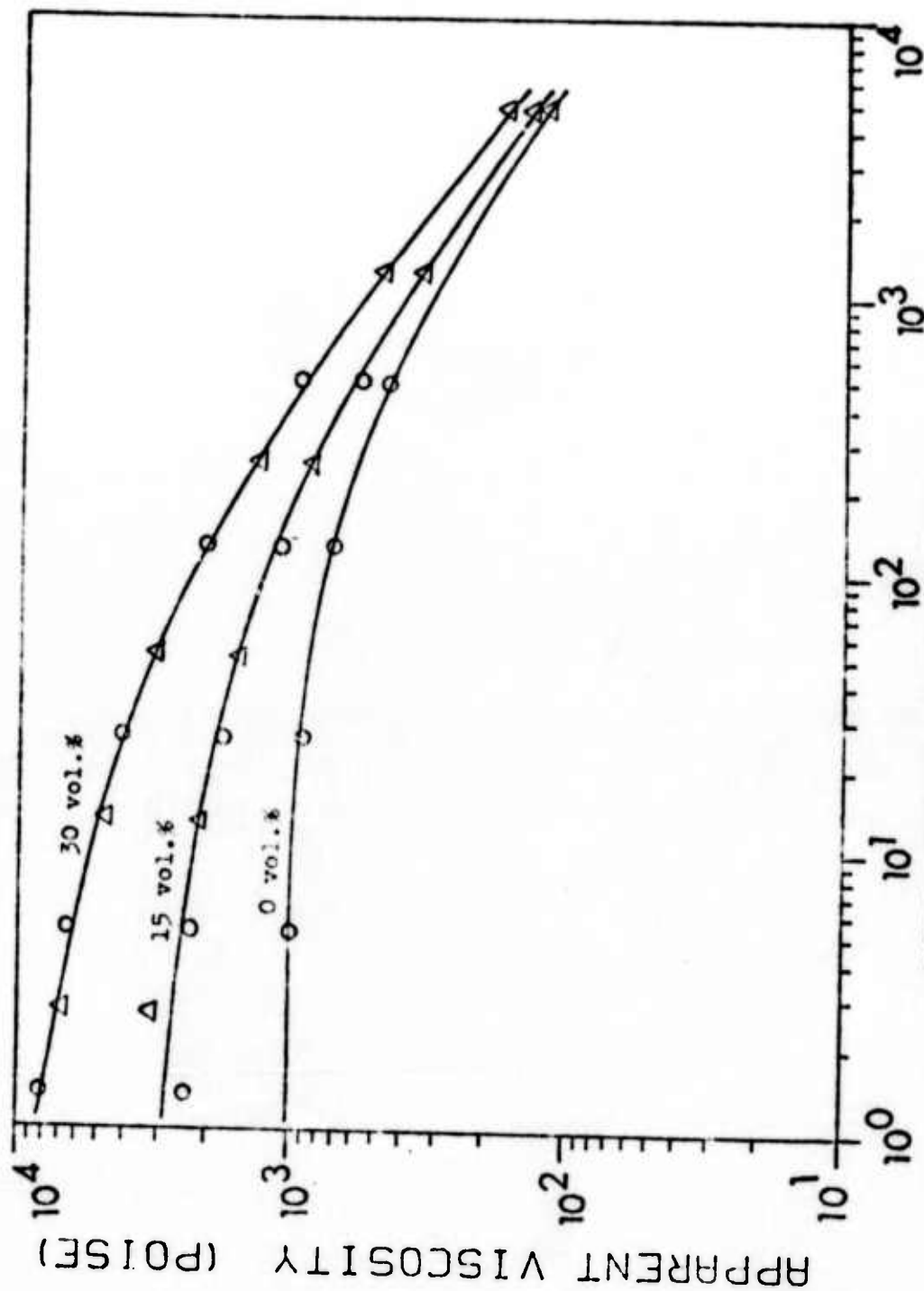


Figure 7 Viscosity-shear rate behavior of three suspensions of fibers in 1000 P oil. The symbols (\circ -1/4" cap.; Δ -1/8" cap.) represent $\pm 6\%$ error flags.

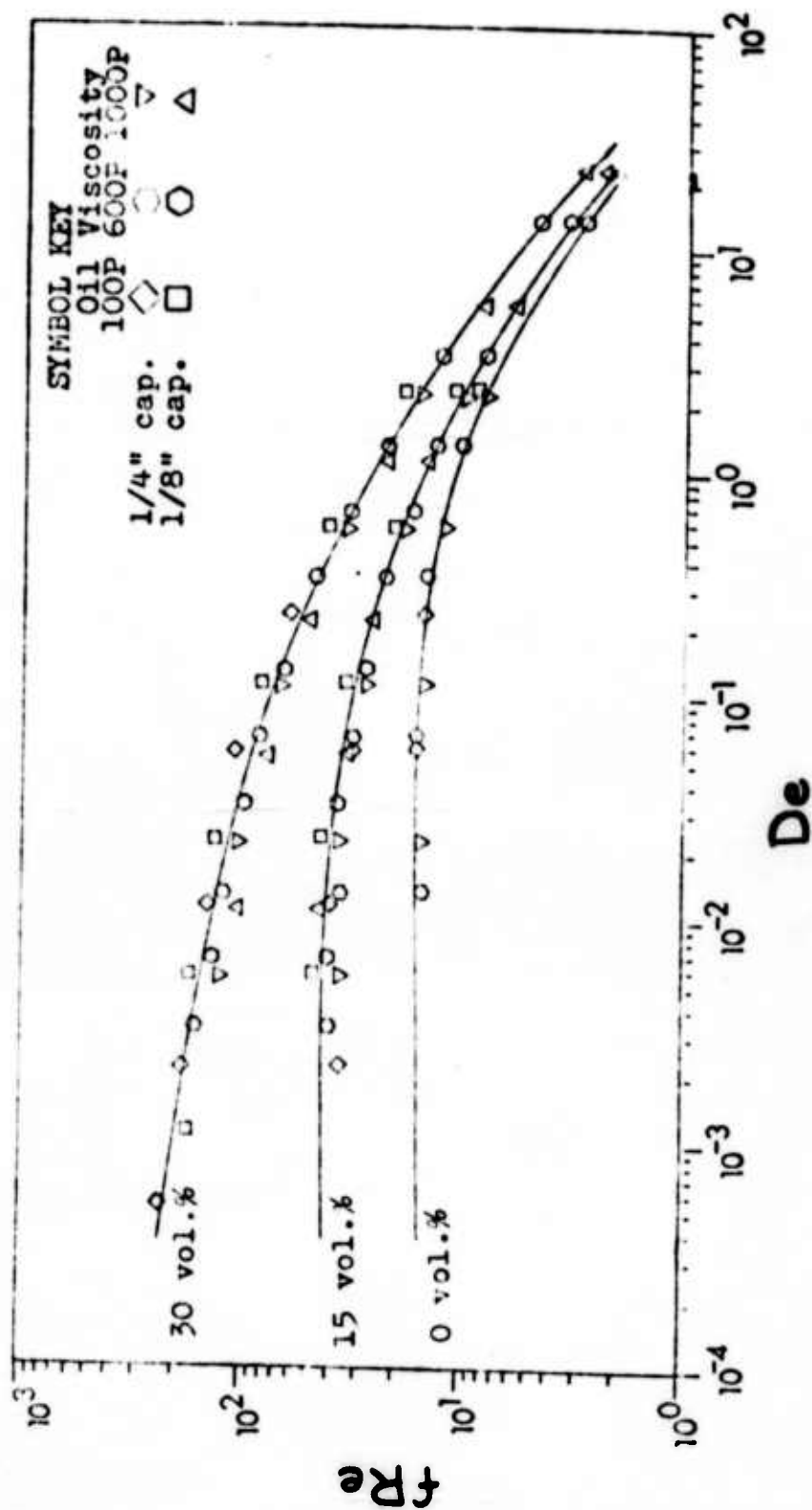


Figure 8. Plot of the dimensionless groups of the system at constant n . Symbol size represents $\pm 5\%$ error flags.

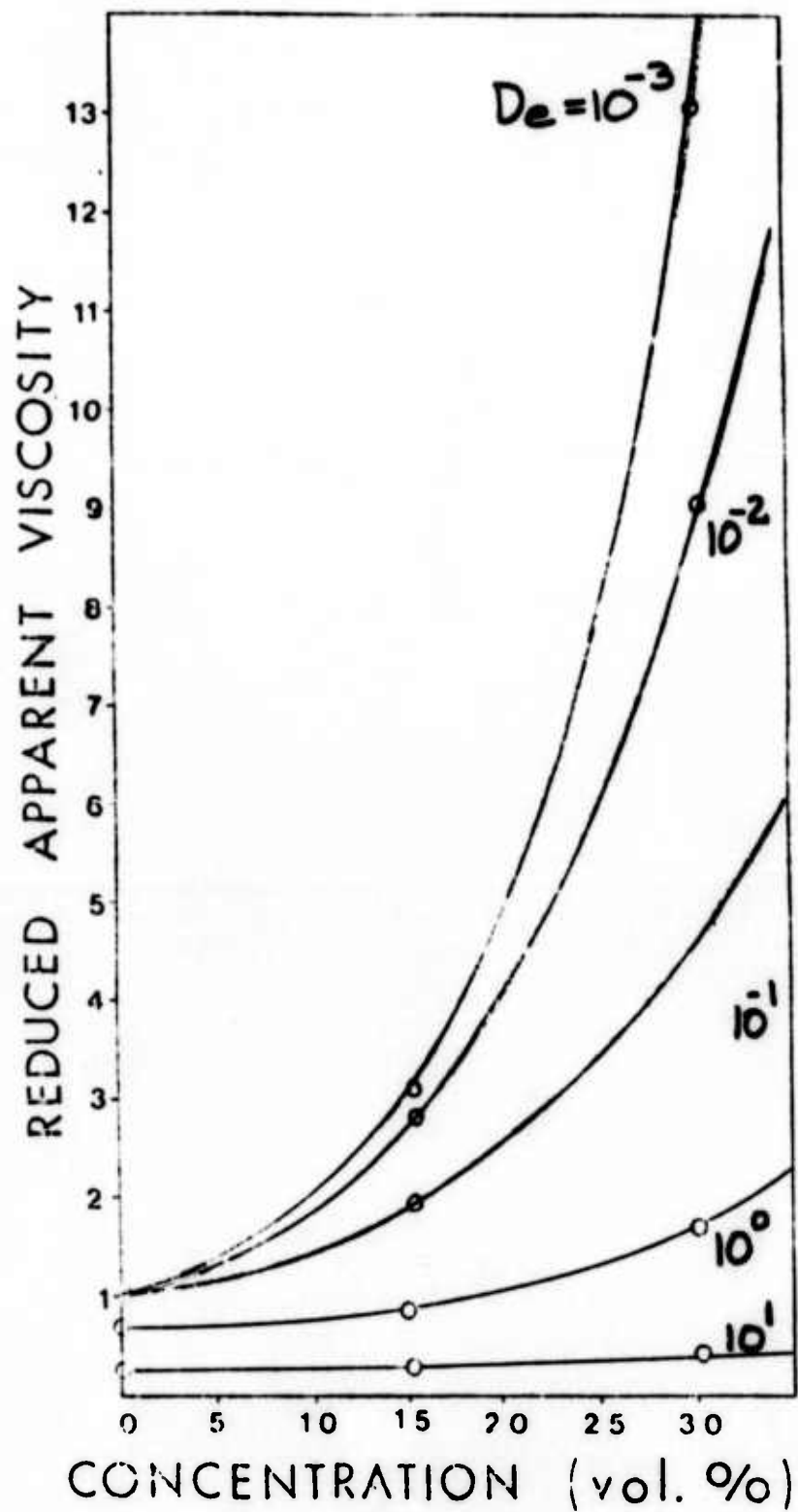


Figure 9. Reduced viscosity-concentration dependence of all suspensions at several Deborah numbers. The symbols have no significance as error flags.

28

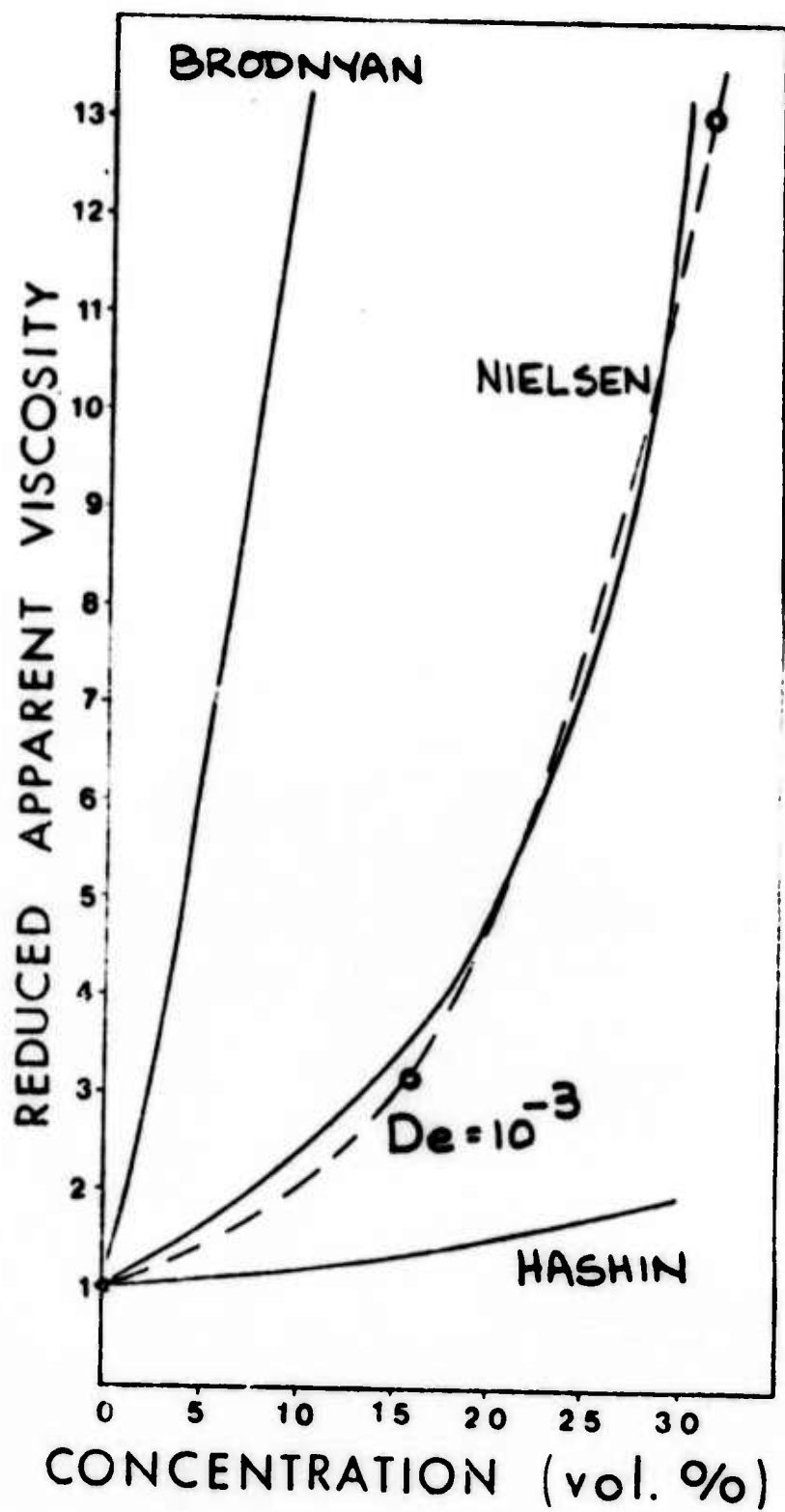


Figure 10. Comparison of viscosity-concentration dependence at lowest Deborah number with literature predictions.

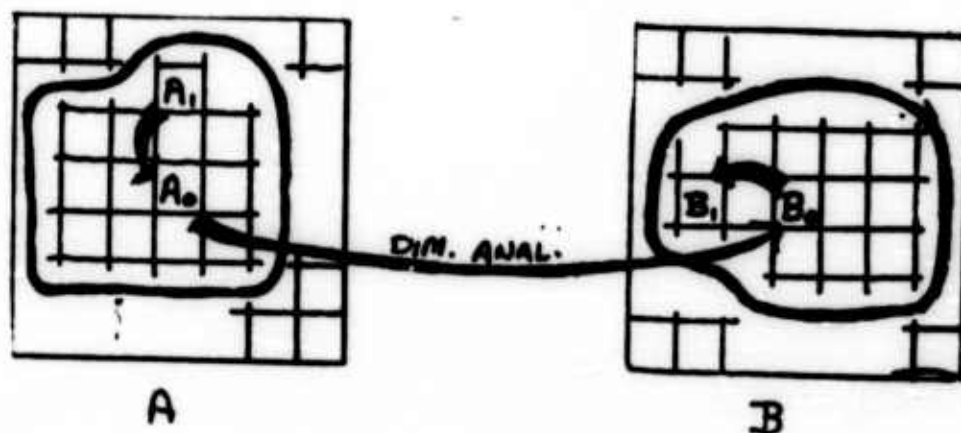


Figure 11. Representations of the ensembles of all possible initial fiber position distributions for two suspensions with different oil viscosities. Each small square represents a particular distribution. The distributions inside the closed curve are experimentally indistinguishable.